Core and Corona Structure of Mixed Polymeric Micelles

Ilja K. Voets,* Arie de Keizer, and Martien A. Cohen Stuart

Laboratory of Physical Chemistry and Colloid Science, Wageningen University, Dreijenplein 6, 6703 HB Wageningen, The Netherlands

Pieter de Waard

Wageningen NMR Centre, Wageningen University, Dreijenlaan 3, 6703 HA Wageningen, The Netherlands

Received May 1, 2006; Revised Manuscript Received June 23, 2006

ABSTRACT: Mixed polymeric micelles have been prepared from aqueous solutions of poly(2-(dimethylamino)-ethyl methacrylate)-*block*-poly(glyceryl methacrylate), $PDMAEMA_{45}$-*b*-$PGMA_{90}$, and poly(acrylic acid)-*block*-poly(acrylamide), PAA_{42}-*b*-$PAAm_{417}$, through complex coacervation of the oppositely charged blocks. Rather monodisperse, spherical aggregates are formed with a $R_h = 15.2 \pm 0.4$ nm. The extent of chain mixing between poly(acrylic acid) and poly(2-(dimethylamino)ethyl methacrylate) in the micellar core and poly(acrylamide) and poly(glyceryl methacrylate) in the micellar corona has been investigated by 2D ^{1}H NMR NOESY experiments. The presence of cross-peaks for protons in different core and corona blocks indicates that the two blocks are in close proximity (<0.5 nm) and micelles are formed in which both core and corona are mixed.

Introduction

Structure and morphology of polymeric micelles is an active branch of colloid science.[1,2] In recent years, a combination of several types of associative and/or segregative microphase separation has been used to form a variety of complex and hierarchical morphologies consisting of more than two domains, by segregation inside the core or the shell. Several approaches have been used to form micelles with multidomain cores, such as onion-type micelles[3−6] and multicompartment micelles involving di- and triblock copolymers,[7] as well as mikto arm stars.[8] Multidomain shell structures,[9−12] including vesicles[13−16] with phase-separated solvent-soluble blocks, one residing inside and one outside the vesicle wall, have also been reported by several groups.

It is well-known that two polymers in a common (good) solvent usually segregate. Despite the current interest in multidomain micelles, there have been very limited studies on the extent of chain mixing in a micellar corona on a molecular level.[2] In this work, we present 2D ^{1}H NMR NOESY experiments that measure polymer chain mixing in situ in both micellar core and corona. In principle, this technique can be applied to any kind of self-assembled structure, for any geometry (i.e., globules, vesicles, rods, etc.) or type of constituent (i.e., low-molecular-weight surfactants, high-molecular-weight amphiphiles forming conventional block copolymer micelles with a hydrophobic core). However, the 2D NOESY technique probes internuclear distances (typically <0.5 nm) only if the protons maintain sufficient rotational mobility within the aggregate, as the degree of peak broadening is inversely proportional to the rotational mobility.

We prepared so-called complex coacervate core micelles (C3Ms)[1,17,18] of poly(2-(dimethylamino)ethyl methacrylate)-*block*-poly(glyceryl methacrylate), $PDMAEMA_{45}$-*b*-$PGMA_{90}$, and poly(acrylic acid)-*block*-poly(acrylamide), PAA_{42}-*b*-$PAAm_{417}$ (1 mM $NaNO_3$, pH = 6.7, 25 °C), consisting of a complex coacervate core (PAA_{42} + $PDMAEMA_{45}$) and a water-swollen corona ($PAAm_{417}$ + $PGMA_{90}$). Other terms used to denote this type of micelle are polyion complex micelles,[14] block ionomer complex micelles, or interpolyelectrolyte complexes (IPEC).[3] Dynamic light scattering has been used to investigate the overall micellar characteristics, such as hydrodynamic radius (R_h), and the extent of core and corona chain mixing (Figure 1) has been studied by 2D ^{1}H NMR NOESY experiments.

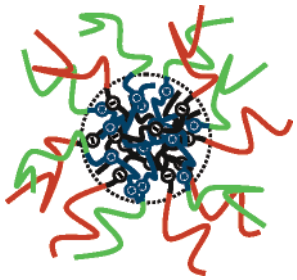

Figure 1. Schematic representation of polymer chain mixing in the core and corona of complex coacervate core micelles consisting of $PDMAEMA_{45}$-*b*-$PGMA_{90}$ and PAA_{42}-*b*-$PAAm_{417}$.

Experimental Section

Materials. Poly(acrylic acid)-*block*-poly(acrylamide), PAA_{42}-*b*-$PAAm_{417}$, synthesized according to the MADIX process,[19] has been kindly provided by Rhodia. Poly(2-(dimethylamino)ethyl methacrylate)-*block*-poly(glyceryl methacrylate), $PDMAEMA_{45}$-*b*-$PGMA_{90}$, was synthesized as described previously.[20] (The subscripts correspond to the degree of polymerization.) Figure 2 depicts the chemical structure of the diblock copolymers used in this study.

Aqueous solutions of micelles were prepared by mixing of polymer stock solutions at a molar fraction, f_+, of 0.5. The molar fraction denotes the ratio of positively chargeable monomers to total amount of chargeable monomers in solution (f_+ = [PDMAEMA]/[PDMAEMA + PAA]). Typical concentrations of the polymer solutions are on the order of several (LS) to several tens (^{1}H NMR) of millimoles per liter, expressed in terms of monomer concentration. Aqueous solutions of the polymers were prepared by dissolution of known amounts of polymer into deionized water or commercial heavy water for the ^{1}H NMR experiments, followed by a pH adjustment using NaOH and HNO_3. Unless otherwise

* Corresponding author. E-mail: ilja.voets@wur.nl.

10.1021/ma060965o CCC: $33.50
Published on Web 08/01/2006

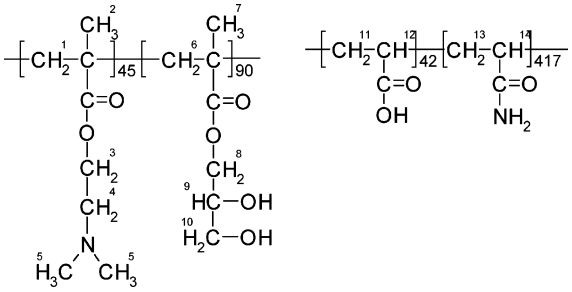

Figure 2. Chemical structures of the diblock copolymers used in this study: $PDMAEMA_{45}$-*b*-$PGMA_{90}$ (left) and PAA_{42}-*b*-$PAAm_{417}$ (right). The numbers beside the brackets denote the degree of polymerization. The numbers 1−14 correspond to the chemical shifts listed in Table 1.

specified, all experiments were performed at 1 mM $NaNO_3$ and 25.0 °C.

Dynamic Light Scattering. Light scattering measurements were performed with an ALV light scattering apparatus, equipped with a 400 mW argon ion laser operated at a wavelength of 514.5 nm. A refractive index matching bath of filtered *cis*-decalin surrounded the cylindrical scattering cell, and the temperature was controlled at 25.0 ± 1.0 °C using a Haake C35 thermostat. Total static light scattering intensity (I) and the second-order correlation function $G_2(t)$ were recorded as a function of scattering angle (70°−120°).

The second-order correlation function $G_2(t)$ can be expressed in the first-order correlation function $G_1(t)$ according to the Siegert relation:

$$G_2(t) = B(1 + \beta G_1(t)^2) \tag{1}$$

where B is the baseline constant and β is an optical constant. In the case of a perfect setup, both equal unity.

In the case of single-exponential decay, $G_1(t)$ can be expressed in terms of a typical decay rate Γ and time t.

$$G_1(t) = e^{-\Gamma t} \tag{2}$$

The apparent translational diffusion coefficient D_a is given by eq 3:

$$\Gamma = D_a q^2 \tag{3}$$

where q is the absolute value of the scattering vector

$$q = (4\pi n \sin(\theta/2))/\lambda \tag{4}$$

where n is the refractive index of the solvent, θ is the scattering angle, and λ is the wavelength of the incident light.

For spherical particles, the translational diffusion coefficient can be related to the hydrodynamic radius R_h according to the Stokes−Einstein equation:

$$D_a = k_B T/(6\pi\eta R_h) \tag{5}$$

where k_B is the Boltzmann constant, T is the absolute temperature, and η is the viscosity of the solvent.

DLS measurements have been analyzed according to standard methods (method of cumulants[21] using standard ALV software and CONTIN[22,23]).

^{1}H NMR. Nuclear Overhauser effect spectroscopy (NOESY) is a two-dimensional NMR technique probing internuclear distances by means of the nuclear Overhauser effect. This effect describes the change in resonance intensity of a proton A due to saturation of a nearby proton B and depends on the fraction of spin−lattice relaxation (T_1) of proton A caused by its dipolar interaction with proton B. The NOE scales with r^{-6}, where r is the internuclear distance between proton A and B, as the relaxation effect is proportional to the square of the dipolar field, which is proportional to r^{-3}. The results of a 2D ^{1}H NMR NOESY experiment are typically presented in a so-called contour plot, where the 1-dimensional ^{1}H NMR spectra are plotted on the vertical and horizontal axis. Nuclear Overhauser effects (NOE's) between protons A and B will appear as a so-called cross-peak on the intersection of two straight lines at the chemical shifts (δ) of protons A and B. Cross-peaks between two unlike protons, i.e., two protons that differ in chemical shift, are necessarily off-diagonal, but symmetrical with respect to the diagonal. In other words, a cross-peak between protons A and B appears at the intersection of $\delta_{x,A}$ and $\delta_{y,B}$ and of $\delta_{x,B}$ and $\delta_{y,A}$. A more extensive introduction to 2D ^{1}H NMR NOESY can be found elsewhere.[24,25]

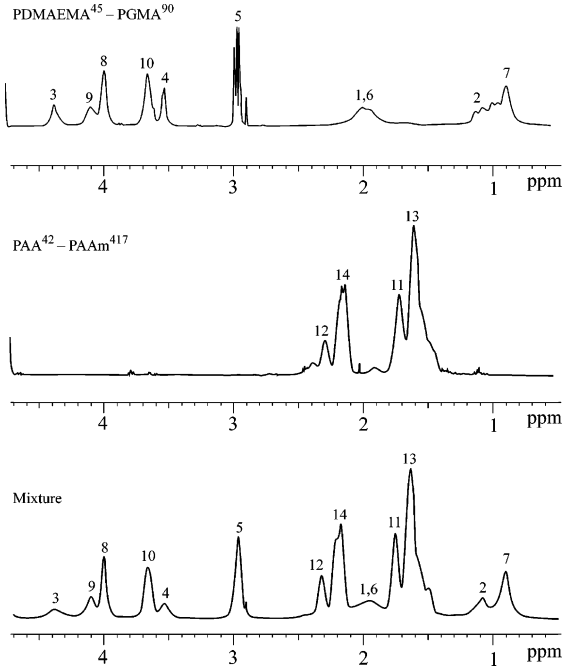

Figure 3. ^{1}H NMR spectra for solutions of $PDMAEMA_{45}$-*b*-$PGMA_{90}$ (upper panel), PAA_{42}-*b*-$PAAm_{417}$ (middle panel), and their mixture (lower panel) in D_2O.

Table 1. Chemical Shifts (δ in ppm) for Solutions of PAA_{42}-*b*-$PAAm_{417}$, $PDMAEMA_{45}$-*b*-$PGMA_{90}$, and Their Mixture (Complex Coacervate Core Micelle)

	chemical shift (δ in ppm)		
proton	$PDMAEMA_{45}$-*b*-$PGMA_{90}$	PAA_{42}-*b*-$PAAm_{417}$	micelle
1	1.95[a]		1.96
2	1.08[a]		1.08
3	4.38		4.37
4	3.53		3.54
5	2.96		2.96
6	1.95[a]		1.96
7	0.90		0.90
8	4.00		4.00
9	4.10		4.10
10	3.64		3.67
11		1.73	1.76
12		2.29	2.32
13		1.61	1.64
14		2.16	2.18

[a] Chemical shift assignment is somewhat arbitrary due to peak overlap (see Figure 3, upper panel).

^{1}H NMR spectra of the individual polymers were recorded at 298 K on a Bruker AMX-400 spectrometer, operating at 400 MHz. ^{1}H NMR spectra of the micellar solutions were recorded at 298 K on a Bruker AMX-500 spectrometer, operating at 500 MHz, located at the Wageningen NMR Centre. For the 2D NOESY spectrum 976 experiments of 2048 data points were recorded, using standard Bruker software. The mixing time was varied in the range 200−1000 ms.

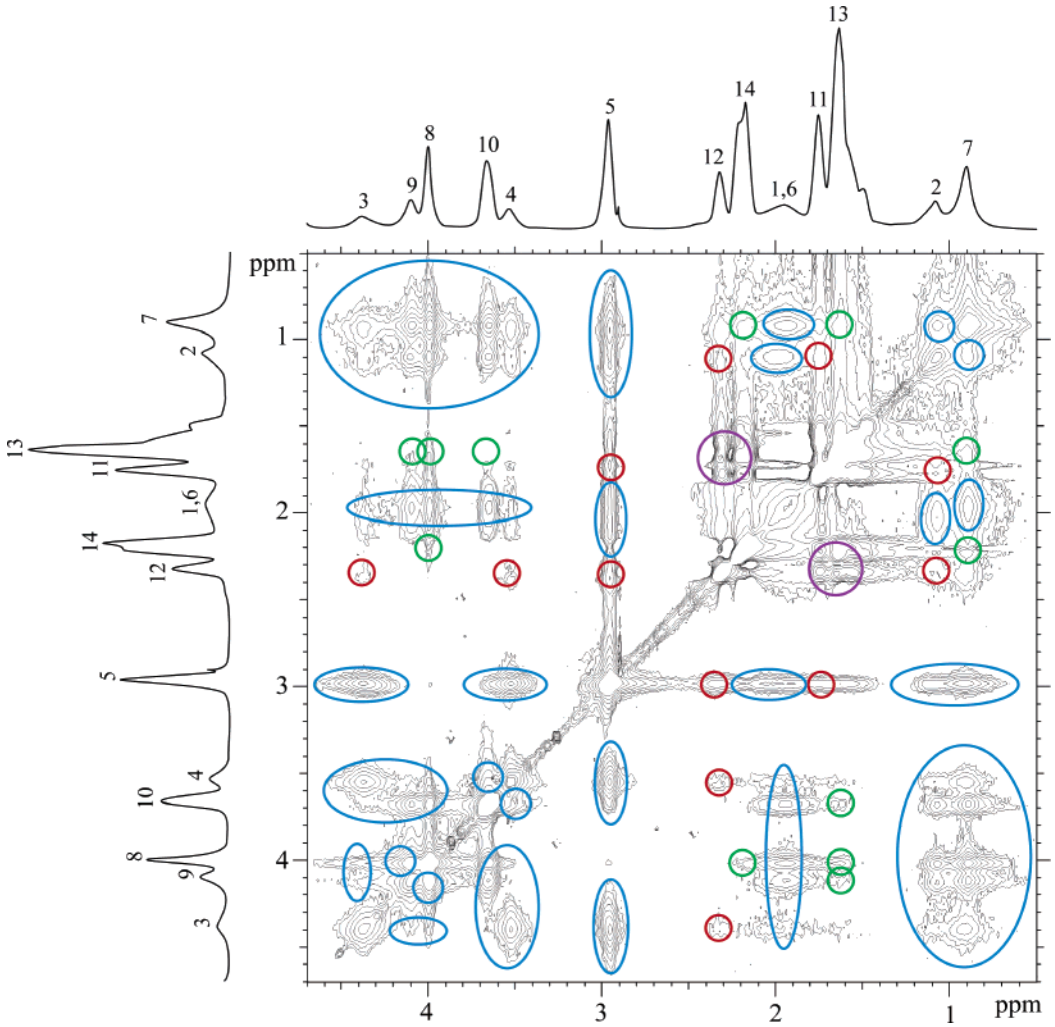

Figure 4. 2D ^{1}H NMR NOESY contour plot of complex coacervate core micelles of PDMAEMA$_{45}$-*b*-PGMA$_{90}$ and PAA$_{42}$-*b*-PAAm$_{417}$ (1 mM $NaNO_3$, pH = 6.7, 25 °C, $f_+ = 0.5$, $C_p = 10$ g/L) in D_2O. Circles indicate intramolecular cross-peaks within PAA$_{42}$-*b*-PAAm$_{417}$ (purple) and PDMAEMA$_{45}$-*b*-PGMA$_{90}$ (blue) as well as intermolecular cross-peaks between core blocks PAA$_{42}$ and PDMAEMA$_{45}$ (red) and corona blocks PAAm$_{417}$ and PGMA$_{90}$ (green).

Results and Discussion

Micellar Characteristics. Upon mixing of PDMAEMA$_{45}$-*b*-PGMA$_{90}$ and PAA$_{42}$-*b*-PAAm$_{417}$ (1 mM $NaNO_3$, pH = 6.7, 25 °C, $f_+ = 0.5$) complex coacervate core micelles are formed, consisting of a complex coacervate core (PAA$_{42}$ + PDMAEMA$_{45}$) and a water-swollen corona (PAAm$_{417}$ + PGMA$_{90}$). From dynamic light scattering measurements, we obtain a value of $R_h = 15.2 \pm 0.4$ nm. The R_h shows a negligible angular and concentration dependence ($0.4 < C_p < 1.5$ g/L, $70° < \theta < 120°$), indicative of a solution of relatively monodisperse, spherical micelles. The reversibility of this type of micelle with respect to mixing fraction, ionic strength, and pH has been discussed previously[1,17] and will be discussed in detail for this particular system in a forthcoming paper.[18] For the present contribution, we will briefly summarize the main characteristics of this relatively novel type of micelle, as they are important for the interpretation of the NMR results.

Contrary to the more traditional hydrophobic core micelles, complex coacervate core micelles are highly penetrated by solvent, in both the core and the corona. The polymer volume fraction will therefore be relatively low, enhancing the mobility of the polymer segments within the whole micelle. The driving force for micellization, electrostatic interaction, is typically weaker than its hydrophobic counterpart, resulting in two important characteristics: a relatively low chain density of polymer chains in the micellar corona, enhancing segment mobility further, and more importantly, the spontaneously formed micelles are reversible stimuli-responsive micelles existing in full thermodynamic equilibrium. They respond reversibly to external stimuli such as mixing fraction, ionic strength, and pH and dissociate when the driving force for micellization is no longer sufficient, for example due to charge screening (above a certain critical ionic strength) or due to low charge densities (above and below a critical pH in the case of weak polyelectrolytes).

Core and Corona Structure. The upper and middle panels in Figure 3 depict the ^{1}H NMR spectra obtained for the individual polymers. Peaks have been assigned (Table 1) on the basis of these spectra.

A comparison has been made between the proton chemical shifts and peak widths for the individual polymer solutions and their mixture. Rather strikingly, the influence of micellization on both the proton chemical shifts and the relative peak widths seems to be negligible, indicating the high polymer flexibility in the complex coacervate core micelle, as described above. No apparent shifts in peak position, indicative of interaction with neighboring protons in the micelle,[26] have been observed.

To study the interactions and 3D spatial correlations between protons in the mixed micelle more directly, we performed 2D ^{1}H NMR NOESY experiments with several mixing times.

Protons that are in close proximity (typically <0.5 nm) will give a symmetric off-diagonal cross-peak in the NOESY contour plot (Figure 4) due to cross-relaxation.

Clearly, several cross-peaks can be distinguished (see also Supporting Information), both intramolecular (blue and purple encircled) and intermolecular (red and green encircled). Naturally, the intramolecular cross-peaks are substantially more pronounced than the intermolecular cross-peaks. Intermolecular correlations are found between protons of the two different core (red circles) and corona (green circles) blocks, with the former being relatively stronger. These results are consistent with and directly show the close spatial correlation due to electrostatic interaction between acidic and basic monomers in the complex coacervate core. Relatively weak, but still visible, are the cross-peaks between the two different corona blocks, of which those between the backbone methylene protons are most pronounced. These results can be interpreted as a consequence of chain mixing between $PAAm_{417}$ and $PGMA_{90}$ in the micellar corona, as shown in the schematic representation of Figure 1. The weak nature of the cross-peaks between the corona blocks reflects the low chain density in the corona (as discussed previously) as well as the difference between the block lengths of $PGMA_{90}$ and $PAAm_{417}$. Upon closer inspection, one can even observe cross-peaks between core and corona blocks, both inter- and intramolecular. The intramolecular NOE interactions are well pronounced, but the intermolecular NOE interactions, except between protons 13 and 5, are extremely weak, and their assignment may be a subject of some debate. This implies that core and corona blocks are not intricately mixed; i.e., the interfacial width between core and corona is not very large. However, we note that this experiment is not well suited to afford such a conclusion due to the inherent low intensity of the NOE interactions.

Conclusions

Mixed polymeric micelles have been prepared from aqueous solutions of $PDMAEMA_{45}$-*b*-$PGMA_{90}$ and PAA_{42}-*b*-$PAAm_{417}$ (1 mM $NaNO_3$, pH = 6.7, 25 °C) through complex coacervation of the polyelectrolyte blocks. Rather monodisperse, spherical aggregates are formed with a $R_h = 15.2 \pm 0.4$ nm. 2D ^{1}H NMR NOESY experiments indicate close proximity between protons of both the core and corona forming blocks, which we interpret as a consequence of mixing of the PAA_{42} and $PDMAEMA_{45}$ blocks in the core and of $PAAm_{417}$ and $PGMA_{90}$ blocks in the corona.

Acknowledgment. This work has been carried out in the framework of the EU Polyamphi/Marie Curie program (FP6-2002, Proposal 505027). One of us was financed by the SONS Eurocores program (Project JA016-SONS-AMPHI). We kindly acknowledge A. Huijbrechts for performing the 1D ^{1}H NMR experiments as well as T. Hellweg and A. Walther for interesting discussions on the light scattering and 2D ^{1}H NMR measurements.

Supporting Information Available: ^{1}H NMR NOESY contour plot of complex coacervate core micelles of $PDMAEMA_{45}$-*b*-$PGMA_{90}$ and PAA_{42}-*b*-$PAAm_{417}$ and tables of intra- and intermolecular NOE interactions in complex coacervate core micelles of $PDMAEMA_{45}$-*b*-$PGMA_{90}$ and PAA_{42}-*b*-$PAAm_{417}$. This material is available free of charge via the Internet at http://pubs.acs.org.

References and Notes

(1) Cohen Stuart, M. A.; Hofs, B.; Voets, I. K.; de Keizer, A. *Curr. Opin. Colloid Interface Sci.* **2005**, *10*, 30−36.
(2) Fustin, C. A.; Abetz, V.; Gohy, J. F. *Eur. Phys. J. E* **2005**, *16*, 291−302.
(3) Pergushov, D. V.; Remizova, E. V.; Gradzielski, M.; Lindner, P.; Feldthusen, J.; Zezin, A. B.; Mueller, A. H. E.; Kabanov, V. A. *Polymer* **2004**, *45*, 367−378.
(4) Prochazka, K.; Martin, T. J.; Webber, S. E.; Munk, P. *Macromolecules* **1996**, *29*, 6526−6530.
(5) Gohy, J. F.; Willet, N.; Varshney, S.; Zhang, J. X.; Jerome, R. *Angew. Chem., Int. Ed.* **2001**, *40*, 3214−3216.
(6) Kriz, J.; Masar, B.; Plestil, J.; Tuzar, Z.; Pospisil, H.; Doskocilova, D. *Macromolecules* **1998**, *31*, 41−51.
(7) Kubowicz, S.; Baussard, J. F.; Lutz, J. F.; Thunemann, A. F.; von Berlepsch, H.; Laschewsky, A. *Angew. Chem., Int. Ed.* **2005**, *44*, 5262−5265.
(8) Li, Z. B.; Kesselman, E.; Talmon, Y.; Hillmyer, M. A.; Lodge, T. P. *Science* **2004**, *306*, 98−101.
(9) Gohy, J. F.; Khousakoun, E.; Willet, N.; Varshney, S. K.; Jerome, R. *Macromol. Rapid Commun.* **2004**, *25*, 1536−1539.
(10) Erhardt, R.; Boker, A.; Zettl, H.; Kaya, H.; Pyckhout-Hintzen, W.; Krausch, G.; Abetz, V.; Mueller, A. H. E. *Macromolecules* **2001**, *34*, 1069−1075.
(11) Erhardt, R.; Zhang, M. F.; Boker, A.; Zettl, H.; Abetz, C.; Frederik, P.; Krausch, G.; Abetz, V.; Mueller, A. H. E. *J. Am. Chem. Soc.* **2003**, *125*, 3260−3267.
(12) Sfika, V.; Tsitsilianis, C.; Kiriy, A.; Gorodyska, G.; Stamm, M. *Macromolecules* **2004**, *37*, 9551−9560.
(13) Liu, F. T.; Eisenberg, A. *J. Am. Chem. Soc.* **2003**, *125*, 15059−15064.
(14) Schrage, S.; Sigel, R.; Schlaad, H. *Macromolecules* **2003**, *36*, 1417−1420.
(15) Stoenescu, R.; Meier, W. *Chem. Commun.* **2002**, *24*, 3016−3017.
(16) Luo, L. B.; Eisenberg, A. *Angew. Chem., Int. Ed.* **2002**, *41*, 1001−1004.
(17) van der Burgh, S.; de Keizer, A.; Cohen Stuart, M. A. *Langmuir* **2004**, *20*, 1073−1084.
(18) Hofs, B.; Voets, I. K.; de Keizer, A.; Cohen Stuart, M. A. *Phys. Chem. Chem. Phys.*, accepted.
(19) Taton, D.; Wilczewska, A. Z.; Destarac, M. *Macromol. Rapid Commun.* **2001**, *22*, 1497−1503.
(20) Hoogeveen, N. G.; Cohen Stuart, M. A.; Fleer, G. J.; Frank, W.; Arnold, M. *Macromol. Chem. Phys.* **1996**, *197*, 2553−2564.
(21) Koppel, D. E. *J. Chem. Phys.* **1972**, *57*, 4814−4820.
(22) Provencher, S. W. *Comput. Phys. Commun.* **1982**, *27*, 229−242.
(23) Provencher, S. W. *Comput. Phys. Commun.* **1982**, *27*, 213−227.
(24) Atkins, P. W. *Physical Chemistry*, 7th ed.; Oxford University Press: Oxford, 2002.
(25) Mo, H. P.; Pochapsky, T. C. *Prog. Nucl. Magn. Reson. Spectrosc.* **1997**, *30*, 1−38.
(26) Wang, T. Z.; Mao, S. Z.; Miao, X. J.; Zhao, S.; Yu, J. Y.; Du, Y. R. *J. Colloid Interface Sci.* **2001**, *241*, 465−468.

MA060965O